Nano Energy 25 (2016) 203–210

Contents lists available at ScienceDirect

Nano Energy

journal homepage: www.elsevier.com/locate/nanoen

Understanding the interactions between lithium polysulfides and N-doped graphene using density functional theory calculations

Li-Chang Yin [a], Ji Liang [a], Guang-Min Zhou [a], Feng Li [a,*], Riichiro Saito [b], Hui-Ming Cheng [a,*]

[a] Shenyang National Laboratory for Materials Science, Institute of Metal Research, Chinese Academy of Sciences, 72 Wenhua Road, Shenyang 110016, China
[b] Department of Physics, Tohoku University, Sendai 980-8578, Japan

ARTICLE INFO

Article history:
Received 26 March 2016
Received in revised form
30 April 2016
Accepted 30 April 2016
Available online 2 May 2016

Keywords:
Lithium-sulfur battery
Shuttling effect
Density functional theory calculation
Nitrogen-doping
Graphene

ABSTRACT

To understand the origin of the cycling performance improvement observed in lithium-sulfur (Li–S) batteries based on N-doped carbon materials, the interactions between lithium polysulfides (LiPSs) and N-doped graphene (N-G) with different doping configurations have been investigated by density functional theory calculations. It has been found that only N-G with clustered pyridinic N-dopants can strongly attract LiPSs with large enough binding energies to effectively anchor the soluble LiPSs, due to (i) an enhanced attraction between Li ions in LiPSs and pyridinic N-dopants and/or (ii) an additional attraction between S anions in LiPSs and Li ions captured by pyridinic N-dopants. This study has, for the first time, provided a fundamental understanding on the origin of the effective anchoring of LiPSs by N-doped carbon materials, which suppresses the shuttling of LiPSs and produces significant improvement in the cycling performance of Li–S batteries. These findings can also guide the design of more effective N-doped carbons or other N-rich materials for Li–S batteries, preventing the undesirable LiPS shuttling.

1. Introduction

Lithium-sulfur (Li–S) batteries are promising and attractive candidates for next generation portable or stationary power supplies due to their high theoretical energy density up to 2600 W h kg^{-1} [1–4]. Although Li–S batteries have been extensively studied during the past three decades [5–18], their practical application is still hindered by the rapid capacity decay and serious self-discharge caused by the dissolving and shuttling of soluble lithium polysulfides (LiPSs) in electrolytes [19–22]. The shuttling occurs when the interactions between LiPSs and the commonly used electrolyte solvents (*e.g.* 1, 2-dimethoxyethane (DME) and 1,3-dioxolane (DOL)) are stronger than those between LiPSs and electrode materials. In order to avoid the shuttling effect, carbon materials have been widely used in Li–S batteries not only as conductive additives, but also as spatial confiners, and anode protectors [23–26]. In particular, N-doped carbon was found to be able to anchor LiPSs [27–32], thus suppressing their shuttling and improving the cycling performance of a Li–S battery. For example, it was reported that N-doped graphene (N-G) with pyrrolic and pyridinic N-dopants could bind LiPSs more strongly with larger binding energies (E_b) than pristine graphene (p-G) [27–30]. An amino-functionalized reduced graphene oxide (r-GO) was also reported to be able to stabilize both sulfur and LiPSs by covalent bonding [33]. In addition, phosphorene was recently predicted to be a promising host to anchor LiPSs for Li–S battery cathodes [34]. However, considering (i) the many possible doping configurations that may exist in N-G and (ii) the difficulty of controlling the synthesis of N-G with specific doping configurations, it would be difficult to validate experimentally which doping configuration in N-G works as an effective immobilizer for LiPSs in a Li–S battery. Therefore, it is practically important to theoretically investigate the interactions between N-G with different doping configurations and the soluble LiPSs to obtain the optimal design of N-doped carbons for Li–S batteries.

In this paper, a systematic density functional theory (DFT) study has been performed to understand the interactions between LiPSs and N-doped carbon, using N-G with different doping configurations as model materials. A van der Waals (vdW) correction is incorporated in the DFT calculation to calculate the E_b between LiPSs and N-G with different doping configurations, including isolated/clustered amino, graphitic, pyridinic, and pyrrolic N-dopants, for obtaining the intrinsic roles of different N-doping configurations on the suppression of the LiPSs shuttling in a Li–S battery.

Our DFT results show that, except for graphitic N, other isolated N-dopants bind LiPSs more or less stronger than p-G. The calculated E_b between LiPSs and isolated amino, graphitic, pyrrolic, or

* Corresponding authors.
E-mail addresses: fli@imr.ac.cn (F. Li), cheng@imr.ac.cn (H.-M. Cheng).

http://dx.doi.org/10.1016/j.nanoen.2016.04.053
2211-2855/

pyridinic N-dopant (0.56–1.18 eV) is smaller than or comparable to those between LiPSs and electrolyte solvent molecules (DME and DOL) (0.87–0.98 eV). This implies an insignificant effect of an isolated N-dopant on the suppression of LiPSs shuttling. On the other hand, it is found that a cluster of pyridinic N-dopants strongly binds to LiPSs with larger binding energies (1.23–3.57 eV) than those between LiPSs and electrolyte solvents. Consequently, clustered pyridinic N-dopants in N-G are effective immobilizers of soluble LiPSs, contributing to the cycling performance improvement of Li–S batteries using N-doped carbons in the cathodes.

2. Computational methods

DFT calculations were performed using the projector augmented wave method [35,36] and a plane-wave (PW) basis set as implemented in the Vienna *ab-initio* simulation package [37]. The Perdew-Burke-Ernzerhof functional [38] for the exchange-correlation term was used for all calculations. The energy cutoff for the PW basis set was set to be 400 eV. Spin polarized calculations were performed for systems with an odd number of electrons. A large poly-aromatic hydrocarbon (PAH) molecule of $C_{96}H_{24}$ was used to represent graphene in a $30 \times 30 \times 20$ Å^3 supercell. Several N-Gs with different N-doping configurations were considered by substituting, removing, and/or adding relevant atoms based on the PAH molecule. Only the Γ point was used to sample the first Brillouin zone of this supercell for all calculations. For the geometry relaxations and energy calculations, vdW interactions were incorporated by the optB88 exchange functional [39,40], and this proved to be very important to accurately evaluate the interactions between S-containing clusters and pristine graphene [41]. All atoms are allowed to be fully relaxed in the fixed $30 \times 30 \times 20$ Å^3 supercell until the residual force per atom decreases to below 0.01 eV Å^{-1}. The charge population was calculated by using Bader charge analysis [42,43]. In order to check the size and edge effects of the finite cluster, we also calculated the E_b by using a larger PAH molecule of $C_{222}H_{42}$ with six hydrogen terminated armchair edges and a periodic structure (a $7 \times 7 \times 1$ supercell with a $2 \times 2 \times 1$ Γ-centered k-mesh). The difference in E_b between Li_2S and p-G/N-G using different structures (*e.g.* $C_{96}H_{24}$, $C_{222}H_{42}$, and the $7 \times 7 \times 1$ periodic structure) is less than 20 meV, which clearly shows that both the size and edge effects are negligible compared with the value of E_b between Li_2S and p-G based on $C_{96}H_{24}$ (480 meV).

3. Results and discussion

Several S-containing clusters, including S_8, Li_2S and Li_2S_{2n} ($n=1$, 2, 3, and 4), were considered in this work to investigate the interactions between sulfur/LiPSs and N-G/p-G. The optimized molecular structures of these clusters in their ground states are shown in Fig. 1. S_8 has a puckered ring structure with the D_{4d} symmetry, and the S–S bond length and S–S–S bond angle were calculated to be 2.10 Å and 109.1°, respectively. As for LiPSs, both Li_2S and Li_2S_2 have C_{2v} symmetry, while other LiPSs have C_2 symmetry due to the lack of mirror symmetry. The shortest Li–S bond length in each molecule increases with increasing cluster size: 2.09 Å for Li_2S, 2.23 Å for Li_2S_2, and 2.36 (2.35 and 2.38) Å for Li_2S_4 (Li_2S_6 and Li_2S_8), while the bond angle of Li–S–Li decreases: 131.9° for Li_2S, 96.8° for Li_2S_4, and 73.5° (69.1° and 66.3°) for Li_2S_4 (Li_2S_6 and Li_2S_8). The calculated S–S bond lengths of Li_2S_4 are 2.13 Å for S_1–S_3 (S_3–S_4) and 2.17 Å for S_2–S_3, larger than that of S_8 (2.10 Å) due to the less covalent character. The calculated S–S bond lengths of Li_2S_6 are 2.12, 2.11 and 2.14 Å for S_1–S_2 (S_5–S_6), S_2–S_3 (S_4–S_5) and S_3–S_4, respectively. The S–S bond lengths of Li_2S_8 are 2.11, 2.13, 2.09 and 2.14 Å for S_1–S_2 (S_7–S_8), S_2–S_3 (S_6–S_7), S_3–S_4 (S_5–S_6) and S_4–S_5, respectively. The optimized structures of S_8, Li_2S and Li_2S_{2n} ($n=1$, 2, 3, and 4) obtained in this work are consistent with the previous calculations [44–46].

When a N atom is doped into graphene, there are three common bonding configurations in the carbon lattice, that is, graphitic N (N_C), pyridinic N (N_{PD}), and pyrrolic N (N_{PL}) [47–55], as shown in Fig. 2. Additionally, amino N with two possible doping configurations, *e.g.* the NH_2 group located at the edge (N_A) or on the basal plane ($N_{A'}$) of graphene as shown in Fig. 2, can be introduced into N-G by reducing graphene oxide under N-containing environments [56,57]. Interestingly, two graphitic N-dopants (N_{2C}) have been observed to preferably occupy the same sub-lattices of graphene synthesized by chemical vapor deposition (CVD) [58,59]. Besides, N_{2PD} (N_{2PL}) denotes two neighboring pyridinic (pyrrolic) N atoms bonding into two adjacent six (five) member rings. It was also reported that native point defects (especially vacancies) and N-dopants (like N_{PD} and N_{PL}) attract each other and prefer to exist together in carbon nanomaterials, resulting in complex doping configurations with clustered N-dopants [60–63], such as two pyridinic plus one pyrrolic N ($N_{2PD/PL}$), three pyridinic N (N_{3PD}), three pyrrolic N (N_{3PL}), and four pyridinic N (N_{4PD}) dopants (Fig. 2). Except for N_{2C} and $N_{A'}$, the other N-dopants are located at edges or defective graphene sites, since the large structural distortion induced by N-doping is possible at these sites [60]. In fact, as shown in Fig. 2, $N_{2PD/PL}$ is composed of one pyrrolic and two pyridinic N atoms with four C vacancies, N_{3PD} consists of three pyridinic N

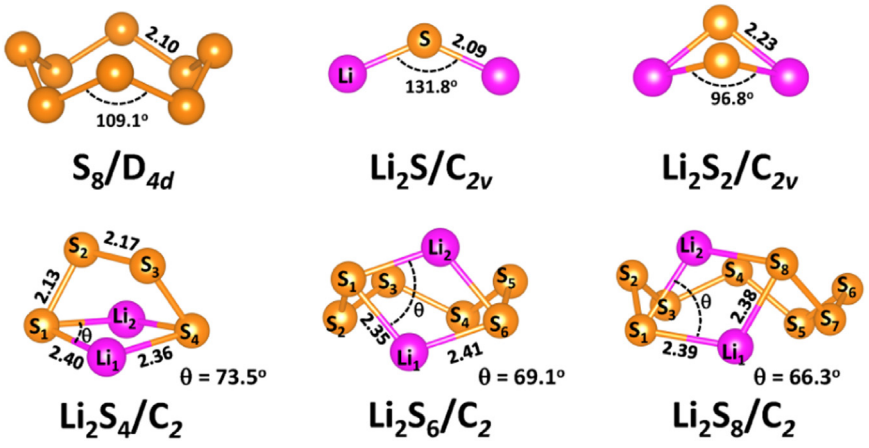

Fig. 1. Fully optimized molecular structures of isolated S_8, Li_2S and Li_2S_{2n} ($n=1$, 2, 3, and 4) clusters in the ground states. The S and Li atoms are denoted by yellow and purple balls, respectively. The symmetry groups, nonequivalent S–S/Li–S bond lengths and S–S–S/Li–S–Li bond angles of each cluster are also listed.